

~~RESTRICTED~~  
~~CONFIDENTIAL~~

COPY NO.  
RM E9C15

CLASSIFICATION CHANGED

NACA RM E9C15

~~RESTRICTED~~

~~CONFIDENTIAL~~  
**NACA**

*naca Release form 603*  
by authority of *H. L. Dryden* Date *June 27, 1951*  
*by HSR, 7-11-51*

~~2703~~  
~~370~~  
~~opt~~  
*copy 2*

# RESEARCH MEMORANDUM

TURBINE-ROTOR-BLADE DESIGNS BASED ON  
ONE-DIMENSIONAL-FLOW THEORY  
I - PERFORMANCE OF SINGLE-STAGE TURBINE  
HAVING 40-PERCENT REACTION

By Robert E. English and Cavour H. Hauser

Lewis Flight Propulsion Laboratory

CLASSIFICATION CANCELLED  
Cleveland, Ohio

Authority *J. W. Crawley* Date *12/14/53*  
*EO 10501*  
By *JH-1-R-54* See *NACA*  
*RF 1907*

UNCLASSIFIED DOCUMENT  
This document contains classified information affecting the National Defense of the United States within the meaning of the Espionage Act, USC 50:31 and 32. Its transmission or the revelation of its contents in any manner to an unauthorized person is prohibited by law. Information so classified may be imparted only to persons in the military and naval services of the United States, appropriate civilian officers and employees of the Federal Government who have a legitimate interest therein, and to United States citizens of known loyalty and discretion who of necessity must be informed thereof.

## NATIONAL ADVISORY COMMITTEE FOR AERONAUTICS

WASHINGTON

June 10, 1949

~~CONFIDENTIAL~~  
UNCLASSIFIED

## NATIONAL ADVISORY COMMITTEE FOR AERONAUTICS

RESEARCH MEMORANDUM

## TURBINE-ROTOR-BLADE DESIGNS BASED ON ONE-DIMENSIONAL-FLOW THEORY

## I - PERFORMANCE OF SINGLE-STAGE TURBINE

## HAVING 40-PERCENT REACTION

By Robert E. English and Cavour H. Hauser

## SUMMARY

As part of a research program to determine **design** criterions for **aircraft** gas turbines with **high efficiency** and high pressure ratio per stage, the **NACA** is investigating a family of **turbine-rotor-blade** designs based on one-dimensional-flow theory and **incorporating systematic changes** in design variables. The rotor blade described herein was designed for a total-to-static pressure ratio of 4.00 and **40-percent** reaction. The static pressure **was** assumed constant along the radius at the entrance and the exit of each row of blades. The rotor-blade passage was based on **one-dimensional-flow** theory. The convex surface of the blade was assigned to be the involute of a circle and the **channel** width was determined from continuity **considerations** by assuming that the drop in static **enthalpy** along the mean flow path of the channel is proportional to the square of the **distance** from the channel entrance.

The performance investigation of this design in an experimental cold-air turbine yielded the following results: The maximum brake internal **efficiency** in the region of the design point was slightly greater than 0.84, and a brake internal efficiency of **0.81 was** obtained for all total-pressure ratios from 1.25 to 3.80. At the equivalent mean blade speed and total-to-static pressure ratio for which the blades were designed, the brake internal efficiency was 0.82. The maximum **brake** net and brake internal efficiencies occurred at blade-to-jet speed ratios between 0.48 and 0.55. Measured static pressures in the **exhaust annulus** showed that, contrary to the design assumption, the static pressure varied 5 percent at the **design** conditions.

~~CONFIDENTIAL~~

UNCLASSIFIED

## INTRODUCTION

As part of a **research program** to establish design criterions for aircraft **gas** turbines with high efficiency and high pressure ratio per stage, a series of turbine-rotor-blade **designs** based on one-dimensional-flow theory and incorporating **systematic changes** in the design variables is being investigated at the **NACA Lewis** laboratory. The same **stator** design will be used throughout the **program**.

The **performance** of one **particular** blade design is reported herein. The general assumptions applicable to all the blade designs together with the features of the particular design are listed. The blades reported herein are identified by a design **reaction** of 40 **percent**, a **suction** (convex) surface contour that is the Involute of **a circle**, a static-enthalpy drop through the rotor blades proportional to the square of the distance **from the channel** entrance measured **along** the flow-path length, and a solidity based on the axial width of 2.2 at the mean radius.

The **performance** of these turbine-blade designs is being **investigated** in an experimental single-stage turbine with entrance conditions of atmospheric **pressure** and a temperature of **710° R**. **Performance** data for the set of blades described herein have been obtained **over** a range of equivalent mean blade speeds from 190 to 807 feet per **second** and total-pressure ratios from 1.18 to 3.80, **which includes** the design values of equivalent mean blade speed and total-pressure ratio of 643 feet per second and 3.32, **respectively**.

Over-all turbine **performance** is presented in the form of a **composite** plot that shows the effect of equivalent mean blade speed and **total-pressure** ratio on the equivalent weight flow, the brake internal efficiency, and the equivalent turbine-shaft work. The **variation** of **brake** internal efficiency with blade-to-jet speed **ratio** is plotted for two **selected values** of total-pressure ratio. **For the same** two values of total-pressure ratio, a **comparison** between brake internal **efficiency** and brake net efficiency is made **over** the full range of blade-to-jet speed ratios. In the blade design, constant static **pressure** along the radius was assumed at the **stator entrance**, the **stator** exit, the rotor **entrance**, and the rotor exit, **which** would result from small **radial** accelerations. The weight flow per unit of **annulus** area was also assumed to be constant in any plane **normal to** the axis of rotation. The difference between the **actual** and theoretical static-pressure distribution **along** the **radius** at the rotor exit **is** presented.

## SYMBOLS

The following symbols are used in this report:

<b>s</b>	velocity of sound, ( <b>ft/sec</b> )
<b>E</b>	turbine-shaft work, ( <b>Btu/lb</b> )
<b>g</b>	standard <b>acceleration</b> due to <b>gravity</b> , 32.17 ( <b>ft/sec<sup>2</sup></b> )
<b>h</b>	<b>specific enthalpy</b> , ( <b>Btu/lb</b> )
<b>J</b>	mechanical equivalent of heat, 778.3 ( <b>ft-lb/Btu</b> )
<b>p</b>	absolute pressure, ( <b>lb/sq ft</b> )
<b>T</b>	absolute temperature, ( <b>°R</b> )
<b>U</b>	mean blade speed, ( <b>ft/sec</b> )
<b>v</b>	absolute velocity of gas, ( <b>ft/sec</b> )
<b>V<sub>j</sub></b>	ideal jet velocity, ( <b>ft/sec</b> )
<b>W</b>	gas velocity relative to rotor, ( <b>ft/sec</b> )
<b>w</b>	weight flow, ( <b>lb/sec</b> )
<b>α</b>	angle of absolute <b>velocity</b> measured <b>from</b> direction of blade motion, ( <b>deg</b> )
<b>β</b>	angle of relative <b>velocity</b> measured <b>from</b> direction of blade motion, ( <b>deg</b> )
<b>η<sub>i</sub></b>	brake internal efficiency
<b>η<sub>net</sub></b>	brake net <b>efficiency</b>
<b>V</b>	ratio of mean blade speed to ideal jet velocity
<b>ρ</b>	mass density, ( <b>slugs/cu ft</b> )

Subscripts:

0	<b>NACA</b> sea-level air; 2116 ( <b>lb/sq ft</b> ); 518.4 ( <b>°R</b> )
1	etator entrance



**Assumptions:**

(1) The total pressure and the total temperature are **uniform** over the blade height at the entrance to the **stator**.

(2) The **expansion** in the turbine is adiabatic.

(3) In any plane **normal** to the axis of rotation, the weight flow per unit radius is proportional to the radius; at **stator entrance, stator exit, rotor entrance, and rotor exit** (stations 1, 2, 3, and 4, respectively), this condition produces constant weight flow per unit of annular **area**.

(4) At **stator entrance, stator exit, rotor entrance, and rotor exit** (stations 1, 2, 3, and 4, respectively), the static pressure is constant along the radius. This assumption produces **constant** resultant velocity  $V_2$  along the radius, which, **according** to reference 1 (p. 146), may be assumed. It is thus assumed that only small radial **accelerations** will be **encountered**.

(5) In the **stator**, the static **pressure** at the exit from the passages between the blades **is** the critical pressure and further expansion with an accompanying **acceleration** to **supersonic** velocities takes place downstream of these passages. For the acceleration beyond sonic **velocity**, the stream does not deflect toward the **axial direction** with the result **that** the absolute velocity at the rotor **entrance**  $V_3$  is at the angle of the trailing edges of the **stator** blades; the increase in flow area required for the supersonic acceleration is obtained **from** a reduction in the **thickness** of the wakes downstream of the trailing edges **of** the **stator** blades.

(6) **In** the rotor blade passage, expansion takes place until critical conditions are obtained unless the assigned amount of reaction is so low that the exit static pressure is greater than the critical pressure in the rotor. When critical conditions are obtained within the rotor-blade passage, the point at which choking **occurs** is made the **passage** exit. **Expansion** takes **place** downstream of the passage to the rotor-exit pressure in the same **manner as** the **supercritical** expansion for the **stator**. The relative velocity at the rotor exit is at the angle of the trailing edges of the rotor blades, which was **calculated** to maintain continuity of flow through the rotor blade passage.

(7) The **velocity** coefficient (ratio of actual to ideal velocity) for the **stator** is 0.965. (See reference 2.)

(8) **In** the rotor, the flow losses **reduce** the exit kinetic energy  $W_4^2/2gJ$  by 3 Btu per pound, a value chosen arbitrarily.

(9) For the combustion products that constitute the working fluid, the ratio of **specific** heats is 1.300, and the specific heat at constant pressure is 0.300. The gas constant for a perfect gas having these properties is 53.9 foot-pounds per pound  $^{\circ}R$ .

These restrictions determine the vector diagram for the turbine. The diagram for the mean **section** of the blade discussed is shown **in** figure 1. The conditions of **constant** angle of flow and constant static pressure along the radius at the rotor **entrance** produce an absolute velocity that is **constant** in both direction and magnitude along the radius.

The turbine design performance for the blade design discussed reduced to **NACA** sea-level **conditions** at the turbine **entrance** is as follows:

Equivalent mean blade speed, $U(a_0/a'_1)$ , ft/sec . . . . .	643
Equivalent weight flow, $w\left(\frac{\rho_0 a_0}{\rho'_1 a'_1}\right)$ , lb/sec . . . . .	5.82
Blade-to-jet speed ratio, $U/v_j$ . . . . .	0.43
Equivalent work output, $E(a_0/a'_1)^2$ , Btu/lb . . . . .	34.8
Total-to-static pressure ratio, $p'_1/p_4$ . . . . .	4.00
Net <b>efficiency</b> . . . . .	0.77

**If** the exit total pressure is determined by adding to the static pressure a dynamic pressure corresponding to the axial component of the **design** exit velocity  $V_{x,4}$ , the total-pressure ratio  $p'_1/p'_4$  **is 3.32 and** the internal **efficiency** is 0.92. **If** the exit total pressure is determined by adding to the static pressure a **dynamic** pressure corresponding to the resultant exit **velocity**  $V_4$ , the internal efficiency is 0.96.

#### Stator Blades

A **single stator** design will be used for the whole series of rotor blades. The **stator** blades were formed from **stampings** of

1/16-inch sheet steel. The profile at the mean section is shown in figure 2. The mean line of the blade profile had a short straight axial section AB. The mean line from B to C was made up of three arbitrary circular arcs of increasing radius. The rest of the mean line from C to D was straight and tangent to the curved section at point c. The geometry of the stator assembly is shown in figure 3; the blades were so mounted that the leading edge was set at an angle of  $14^\circ$  from a radial line through the leading edge of the root section and the trailing edge was set at an angle of  $24^\circ$  from a radial line through the trailing edge of the root section. The blades were first stamped to shape; then the leading edges were rounded to form a 0.062-inch-radius cylinder and the trailing edge was reduced to 0.031 inch as shown in figure 2. The nominal 0.031-inch trailing-edge thickness was slightly and irregularly reduced in the stator blades used in this investigation owing to hand-finishing that was necessitated by mechanical damage to this stator. The curved portion of the blade from B to C was constant over the blade height; but the length AR varied from 0.083 inch at the root section to 0.031 inch at the tip, and the distance CD varied from 0.971 inch at the root section to 1.185 inches at the tip section. This variation in contour from root to tip was made necessary by the assigned angles of  $14^\circ$  and  $24^\circ$  between radial elements and the leading and trailing edges, respectively. The stator-blade height was made equal to the rotor-blade height at the rotor entrance. In order to complete the stator assembly, 36 of these blades were welded to two concentric, cylindrical rings; the fillets thus formed at the roots and the tips of the blades were hand-finished to provide smooth flow passages.

#### Rotor Blades

The rotor-blade profiles at the root, mean, and tip sections of the blade discussed herein were designed in a manner similar to that shown for the mean section in figure 4. An involute of a circle was arbitrarily selected as the part of the suction surface between points A and B. The involute of a circle, which provides the suction surface with a gradually increasing radius of curvature, reduces the magnitude of any decrease in velocity along the suction surface such as might be caused by the combination of a circular arc and a straight line. From the downstream end of the involute (point A, fig. 4) the contour was faired to meet the straight line that extends from E to the trailing-edge circle. Upstream of the involute, the suction surface was faired from point B to the leading-edge circle.

In the entrance region of the rotor cascade immediately upstream of the guided channel ABCDEA, the gas was assumed to turn between  $15^\circ$  and  $20^\circ$  toward the axial direction without changing the magnitude of the relative velocity. This assumption gave the nose of the blade a small angle of attack, which aided in extending the range of efficient operation of the design. (See reference 1, p. 145.)

The pressure (concave) surface of the rotor blades was determined from one-dimensional-flow theory by considering the guided channel ABCDEA between two blades as a curved nozzle for which the specific mass flow on the center line is the average for the channel. For each point Y on the suction surface of the blade, there was a corresponding point Z on the channel center line through which a line passed that was normal to the suction surface. At any point Z along the channel center line for which the channel area is greater than the channel exit area, the ratio of the ideal change in static enthalpy from the entrance of the guided channel to the ideal change in static enthalpy across the rotor was made equal to the square of the ratio of the distance, measured along the suction surface, of the point Y from the entrance of the guided channel to the total channel length from B to E. Downstream of the point at which the channel area became equal to the channel exit area, the area was kept constant; the expansion beyond sonic speed was assumed to take place without loss downstream of the channel. The 3-Btu loss in the rotor was distributed in the following manner: the actual change in static enthalpy to any point Z was assumed to be lower than the ideal change in static enthalpy by an amount proportional to the distance of the point Y from the entrance of the guided channel. A side view of the blade mounted in the wheel is shown in figure 5. The annular area was increased linearly from the entrance to the exit of the rotor by having the annular walls at the inner and outer radii make angles of  $2^\circ 17'$  and  $3^\circ 58'$ , respectively, with the axial direction; The flow was considered to fill the channel at all points. At each of 10 stations in the guided channel ABCDEA (fig. 4), the channel width at point Z satisfying the above conditions was laid off normal to the suction surface. The lines BC and DE were constructed normal to the relative velocities at the entrance and the exit of the guided channel, respectively. The trailing-edge thickness was set at 0.030 inch. The root, mean, and tip sections are superimposed in figure 6 to show the relation among the sections and the general character of the whole blade. The blades had very little twist or change in camber from root to tip.

The turbine wheel was made up of 150 blades that were 1.47 inches long; the mean diameter at the midaxial-width plane was

~~CONFIDENTIAL~~

13.25 inches and the outer wheel diameter was 14.75 inches. The axial clearance between the trailing edge of the **stator** and the leading edge of the rotor was 0.18 inch and the clearance between the rotor blade exit and the downstream guide shells was 0.05 inch. (See fig. 5.) Each blade was made with an integral cap at the tip, so that with the blades clamped between two disks the caps formed a **continuous**, rotating shroud. (See fig. 7.) A cylindrical stationary shroud was used to control leakage past the tips of the rotor blades (fig. 5). The shroud was the same width as the blade caps and the radial **clearance** between the blade caps and the shroud was 0.025 inch or 0.017 of the blade height. Leakage past a shroud of this type is shown in reference 3 to have a small effect on performance.

For the investigation with cold air, the rotor blades used in the turbine were made of die-cast aluminum. **In** the process of manufacture, **unavoidable** errors were introduced, probably **owing** to nonuniform shrinkage of the blade while cooling in the mold. Profiles of sample finished blades were **inspected and** compared with the original blade design. For the blades reported herein, the maximum deviation of the actual blade channel width **from** the design width was less than 4.5 percent of the passage width. The exit angle of the rotor blades was found to be within  $2^\circ$  of the **design** exit angle  $\beta_4$ .

## APPARATUS AND PROCEDURE

### Experimental Equipment and Procedure

For this **investigation**, air **from** the test cell was **used** to operate the turbine. The **air** was drawn through an **electrostatic** precipitator that **removed** foreign material. **In** order to avoid water condensation in the turbine, the filtered air was heated by passing through a thermostatically controlled air heater. **After passing** through the turbine, the air was exhausted by the laboratory low-pressure **exhaust** system. The power output of the **turbine** was **absorbed** by a water brake that was cradle-mounted for torque measurement. A more detailed description of the experimental **equipment** is given in reference 3.

Data were taken at 17 values of total-pressure ratio from 1.18 to 3.80 and at rotative speeds **from** 3880 to 16,490 rpm (**equivalent** mean blade speeds **from** 190 to 807 ft/sec). At each of the 17 pressure ratios, the turbine was operated at 17 rotor speeds with the **exception** of 11 data points at the lowest value of pressure ratio and the higher blade speeds at which the turbine could

produce no shaft power. For all runs, the entrance total temperature was maintained between  $708^{\circ}$  and  $712^{\circ}$  R; the **stator-entrance** total pressure varied between 26 and 29 inches of mercury, depending upon the air flow and local barometric pressure.

### Instrumentation

A cross section of the turbine showing the **instrumentation is** presented in figure 8. Entrance total pressure was indicated by a total-pressure tube 0.75 inch upstream of the **stator** blades; a circumferential and radial total-pressure survey at the **stator** inlet was **made** to insure that this tube indicated the average entrance total pressure. The entrance total temperature was measured with calibrated thermocouples at four stations in a pair of **20-inch-**diameter ducts leading to a plenum **chamber** immediately upstream of the **stator** blades. The rotor-exit static pressure **was** measured with 12 wall taps located 0.72 inch downstream of the rotor, six **on** the inner exhaust-guide shell and six on the **outer** exhaust-guide shell, evenly spaced circumferentially. The exit total temperature was measured with three total-temperature-type thermocouples at the downstream end of the two exhaust-guide shells. Although the temperature variation along the radius may have prevented these thermocouples from accurately indicating an average temperature, the effect on turbine performance **is** small because, in accordance with the manner in which these data were used, **an** error of  $5^{\circ}$  R would change the **computed** Internal or net efficiency less than 0.003.

**Torque** was measured with a commercial springlees dynamometer **scale**. Air flow was **measured** with a submerged 7-inch flat-plate **orifice** upstream of the air heater. Turbine speed was indicated by a calibrated electric **tachometer**.

The instruments were read with the following precision:

- (1) Absolute pressure,  $\pm 0.05$  Inch of **tetrabromoethane**  
(acetylene tetrabromide)
- (2) Temperature,  $\pm 1^{\circ}$  R
- (3) Orifice pressure drop,  $\pm 0.05$  inch of water
- (4) Torque load,  $\pm 0.2$  pound
- (5) Rotatlve **speed**,  $\pm 13$  rpm

The minimum orifice pressure drop was 15 inches of **water** and the **minimum** rotative speed, **3940 rpm**. For a total-pressure ratio of 2.00 or greater, the torque load was at least 25 pounds, and **the maximum** variation and the probable variation in the brake efficiency were 0.018 and less than 0.005, respectively. For total-pressure ratios less than 2.00, the errors in measurement **of** pressure and torque cause the maximum **and** probable **variations in** efficiency to exceed these values; these variations are inversely proportional to the torque load and, roughly, the pressure drop across the turbine.

#### PERFORMANCE CALCULATIONS

Two separate efficiencies **were** determined to express the performance of the turbine. The brake Internal efficiency, which is based on expansion between the entrance and **exit** total pressures, is defined as

$$\eta_i \equiv \frac{E}{(h'_1 - h'_4)_s}$$

where E is the turbine-shaft work. The ideal drop in enthalpy  $(h'_1 - h'_4)_s$  was **computed from** the chart of air properties in reference 4, the values of entrance total pressure and temperature, and the **value** Of **exit total** pressure. The exit total pressure was computed by adding to the measured static pressure a dynamic pressure corresponding to the axial component of the exit velocity computed from continuity **considerations**. The weight flow of air was determined from the orifice measurements together **with** the data of reference 5. This method of computing the **exit** total pressure gives a minimum value because **any** energy available from the tangential component of the **velocity** is neglected.

The brake net efficiency, which is based on **expansion** between the entrance total and exit static pressures, is defined as

$$\eta_{net} \equiv \frac{E}{(h'_1 - h_4)_s}$$

The ideal drop in **enthalpy**  $(h'_1 - h_4)_s$  was computed from the chart of air properties in reference 4, the values **of** inlet total **pres-**sure and temperature, and the value of exit **static** pressure.

Arithmetic averages of the following measurements were used:

- (1) Entrance total temperature, four thermocouples in the pair of ducts leading to the plenum chamber
- (2) Exit total temperature, three thermocouples at downstream end of exhaust-guide shells
- (3) Exit static pressure, twelve wall taps, six in the outer exhaust-guide shell and six in the inner-exhaust guide shell

The ideal jet velocity  $V_j$  is the jet speed for an isentropic expansion from the entrance total state to the exit static pressure, that is,

$$V_j \equiv \sqrt{2Jg (h'_1 - h_4)_s}$$

All turbine performance data were reduced to NACA sea-level air conditions at the turbine entrance. The performance was expressed in terms of the following variables:

- (1) Brake internal efficiency,  $\eta_1$
- (2) Brake net efficiency,  $\eta_{net}$
- (3) Total-pressure ratio,  $p'_1/p'_4$
- (4) Equivalent turbine-shaft work,  $E(a_0/a'_1)^2$
- (5) Ratio of equivalent mean blade speed to equivalent weight flow,  $(\rho'_1/\rho_0) (U/w)$
- (6) Ratio of mean blade speed to ideal jet velocity (blade-to-jet speed ratio),  $\nu$
- (7) Equivalent mean blade speed,  $U(a_0/a'_1)$

## RESULTS AND DISCUSSION

The relation among the brake internal efficiency, equivalent mean blade speed, and total-pressure ratio is presented in figure 9; the symbols represent actual data points. Because the 88

data were obtained at **varying** total-pressure ratios, plots like that of figure 9 are unsuitable for presenting the complete performance; therefore, curves of **constant** equivalent mean blade speed were **faired** through the **computed** data points and **cross-plotted** to present the other performance results.

The over-all turbine performance is presented in figure 10, which is a plot of the equivalent turbine-shaft work against the ratio of equivalent mean blade speed to equivalent Weight **flow**, with equivalent mean blade speed and total-pressure ratio as parameters and with **contours** of brake internal efficiency. **The brake** internal efficiency had a maximum value slightly greater than 0.84 in the region of the **design** point, for which the pressure ratio and blade speed were relatively high. **Another region** of high efficiency occurred at pressure ratios less than 1.50 and equivalent **mean** blade speeds from 300 to 400 feet per second. A maximum efficiency of 0.85 occurred in this region but the pressure ratio and consequently the work output were far below the design values. A brake internal efficiency of 0.81 was obtained over the entire range of total-pressure ratios **from** 1.25 to 3.80. At the equivalent mean blade speed and total-to-static pressure ratio for which the blades were designed, the total-pressure ratio was 3.26; at this point the brake internal efficiency was greater than 0.82, which is 0.10 lower than the design value. The actual total-pressure ratio corresponding to the design total-to-static pressure ratio of 4.00 was 3.26 instead of the **design** value of 3.32 because three operating conditions that differed from the **design conditions** influenced the exit static-to-total pressure ratio: (1) the weight flow, (2) the exit total temperature, and (3) the ratio of specific heats. For a set value of the total-to-static pressure ratio, the **total-pressure** ratio is decreased **for** increased values of Weight **flow** and exit total temperature, but is **increased** for increased values of the ratio of specific heats. The actual weight flow was greater than the design value. Because the efficiency was lower than the design value, the exit total temperature was higher than for the predicted value. The ratio of specific heats was about 1.400 instead of the design value of 1.300. Because the effect of the **greater** weight flow and exit total temperature overbalanced the effect of the change in the ratio of specific heats, the actual total-pressure ratio was lower than the design value.

At the total-pressure ratio of 3.26, the **region** of highest efficiency occurred at equivalent mean blade speeds about 15 percent higher than the design value of 643 feet per second. The increase in brake internal efficiency with higher blade speeds may be attributed to two factors: (1) At the design blade speed, the exit

tangential component of the velocity was appreciable; as the blade speed was increased, the magnitude of this tangential velocity **component** and the loss associated with it were diminished; and (2) as the blade speed was increased, the angle of attack at the rotor entrance **became** smaller. The design angle of attack may have been too large for highest efficiency.

The lines of constant equivalent mean blade speed are vertical above a total-pressure ratio of approximately 2.25 **because** at **these** pressure ratios the **stator** was choking, which resulted in a **constant value** of the ratio of equivalent mean blade speed to equivalent weight flow along the blade-speed curves. At total-pressure ratios less than 2.25, this ratio increased **along lines** of constant blade speed because the weight flow decreased. At the design point, the equivalent weight flow was 5.97 pounds per second, 2.6 percent greater than the design value.

The **variation** of the brake internal efficiency with the **blade-to-jet** speed ratio is **shown** in figure 11 for total-pressure ratios of 1.50 **and** 3.50. **The** highest values of brake internal efficiency were obtained at blade-to-jet speed ratios between 0.48 and 0.55. These **values** were higher than the **design** blade-to-jet speed ratio of 0.43 **because** of the reduction in the exit loss as the blade speed was increased above the design **value**. Blade-to-jet speed ratios greater than 0.55 were unattainable at a total-pressure ratio of 3.50 because of blade-stress **limitations**. **In** general, these curves were **insensitive** to **changes** in total-pressure ratio.

The brake internal and brake net efficiencies are compared in figure 12 for total-pressure ratios **of** 1.50 **and** 3.50. At a total-pressure ratio of 1.50, the brake net efficiency was about 91 percent of the brake internal efficiency, whereas at a total-pressure ratio of 3.50 the ratio of efficiencies was about 0.86. Over the range of blade-to-jet speed ratios, the ratio of the two efficiencies remained practically constant for a given total-pressure ratio because the ratio of exit static-to-total pressures varied only slightly with blade-to-jet speed ratio. The difference between the two efficiencies increased as the total-pressure ratio was increased because at the high total-pressure ratios the large volume of exhaust gas produced high exit **velocities** and consequently a large difference between the **exit** total **and** static pressures. The maximum values of brake net efficiency **were** obtained at **blade-to-jet** speed ratios between 0.48 and 0.55.

**The** relation of brake net efficiency and total-pressure ratio **for** a blade-to-jet speed ratio of 0.54, at which the brake net

efficiency reached its maximum value, is **presented** in figure 13. **At a** total-pressure ratio of 2.70, the brake net efficiency reached the maximum of 0.76.

Although the **turbine** design assumed **constant** static pressure along the **radius** at the **entrance** and the exit of each row of blades, this assumption was not satisfied **in** the actual **turbine**. This deviation **from the design** occurred because the design assumption of constant static pressure along **the** radius **neglected** the radial forces **required** to make a fluid **flow** along a cylindrical surface when high tangential velocities are involved. A measure of the deviation of the actual flow **from the** design flow may be obtained by **comparing** the exit static **pressures** measured at the inner and outer radii. The variation of the static-to-total pressure ratios at the inner and outer radii with total-pressure ratio for the design **equivalent** mean blade speed is shown **in** figure 14. The static **pres-**sure at the **inner** radius was consistently lower than the static pres-  
sure at the outer radius. At a **total-pressure** ratio of 3.26, the average **of** the two static-to-total pressure ratios was 0.25, which **is** the design value, and the variation between the pressures was about 5 percent. **The** pressure variation at the rotor entrance was probably **greater** than 5 percent **because** of the **higher tangential** velocities.

#### SUMMARY OF RESULTS

A set of turbine blades was designed for **40-percent** reaction and a total-to-static pressure ratio of 4.00 based **on** the assumption of constant static pressure along the radius and **one-dimensional-**flow theory for the design of the rotor-blade passages. An inves-  
tigation of this design **in** an **experimental cold-air** turbine yielded the following results:

1. The **maximum** brake **internal efficiency** in the region of **the** design point was slightly greater than 0.84.
2. A brake internal efficiency of 0.81 was obtained over the entire range of total-pressure ratios investigated from 1.25 to 3.80.
3. At the equivalent **mean** blade speed and total-to-static **pres-**sure ratio for which the blades were **designed**, the brake Internal efficiency was greater than 0.82 and the equivalent weight flow was 2.6 percent greater than the design value.

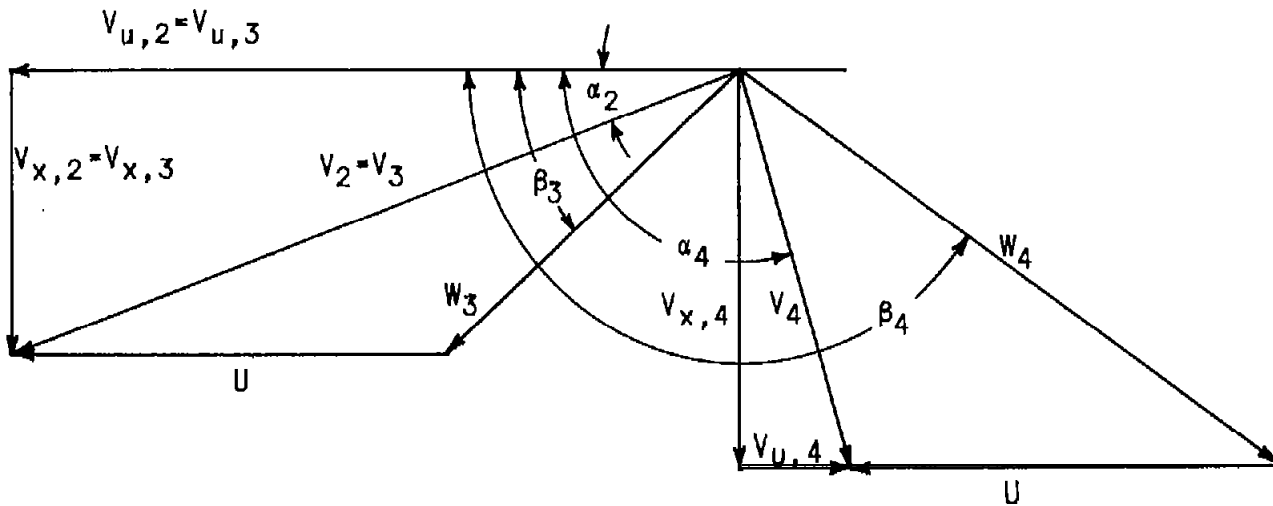
4. The maximum values of both the brake **Internal** efficiency and the brake net efficiency were obtained with blade-to-jet speed ratios between 0.48 and 0.55.

5. Measured static pressures in the **exhaust annulus** showed that, **Contrary to the design assumption**, the static pressure varied **from** root to tip by 5 percent at the design conditions.

Lewis Flight Propulsion **Laboratory**,  
National Advisory **Committee** for Aeronautics,  
**Cleveland**, Ohio.

#### REFERENCES

1. Church, Edwin **F.**, Jr.: **Steam** Turbines. McGraw-Hill Book Co., **Inc.**, 2d ed., 1935, pp. 145, 146.
2. Warren, G. B., and **Keenan**, J. H.: A Machine for Testing **Steam-**Turbine Nozzles by the Reaction Method. Trans. A.S.M.E., vol. 48, 1926, pp. 33-59; **discussion**, pp. 59-64.
3. English, Robert E., **McCready**, Robert J., and McCarthy, John S.: **Some Effects of Stator Cone Angle and Blade-Tip Leakage on** 90-Percent-Reaction Turbine **Having** Rotor-Blade Cape. **NACA RM. ESI21**, 1949.
4. **Amorosi**, A.: Gas Turbine Gas Charts. **Res.** Memo. No. 6-44 (Navehips **250-330-6**), Bur. Ships, Navy Dept., Dec. 1944.
5. Anon.: Fluid Meters, Their Theory and Application. A.S.M.E. Res. Pub., Am. **Soc. Mech. Eng.** (New York), 4th **ed.**, 1937.



	Velocity (ft/sec)		Angle (deg)
"2	2166	$\alpha_2$	20.0
"4	1281	$\alpha_4$	113.2
$V_{u,4}$	506	$\beta_3$	41.9
$V_{x,4}$	1177	84	145.5
$U$	1210		
$W_3$	1110		
$W_4$	2081		



Figure I. - Velocity-vector diagram for mean section of blade for design reaction of 40 percent.

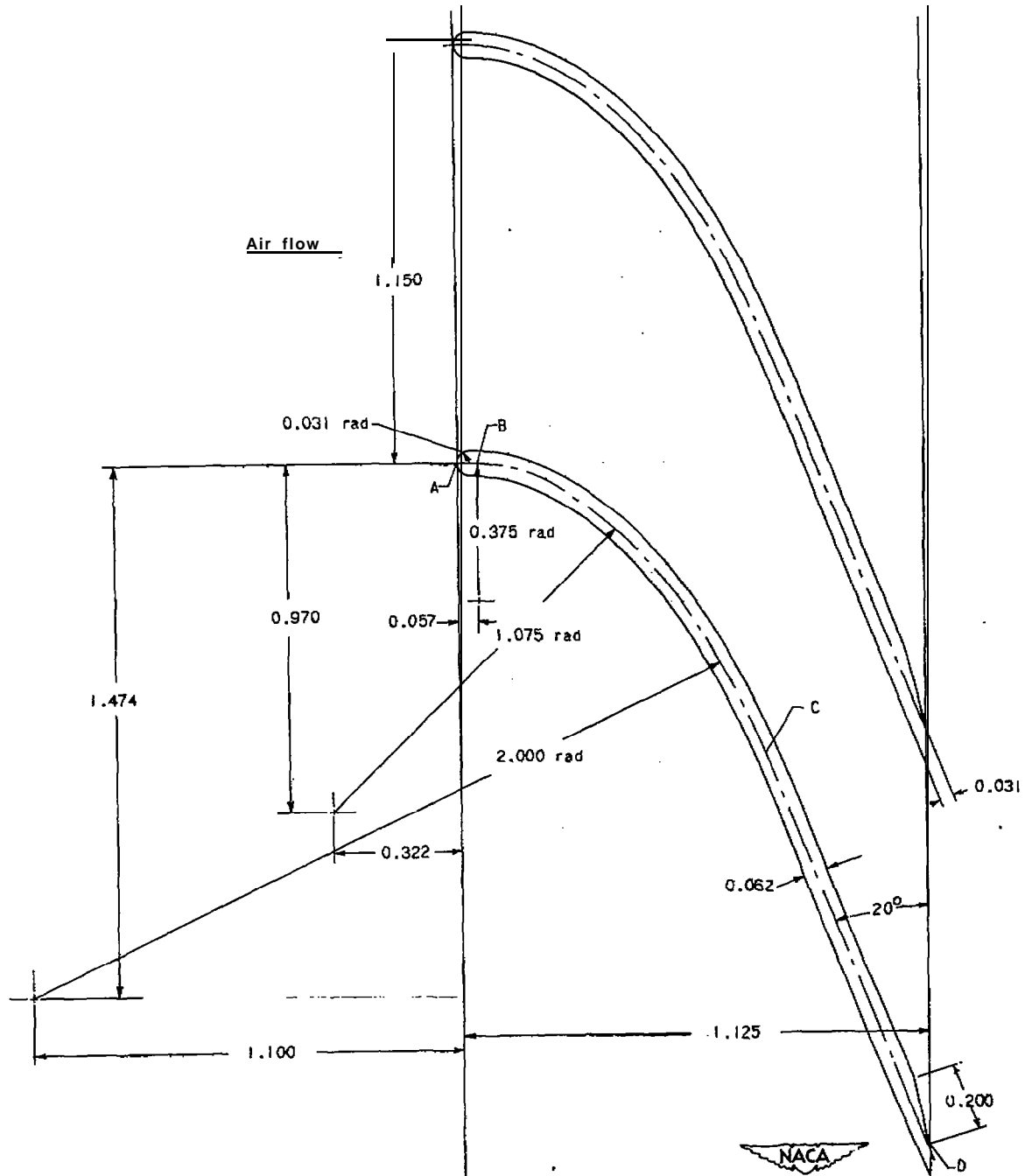
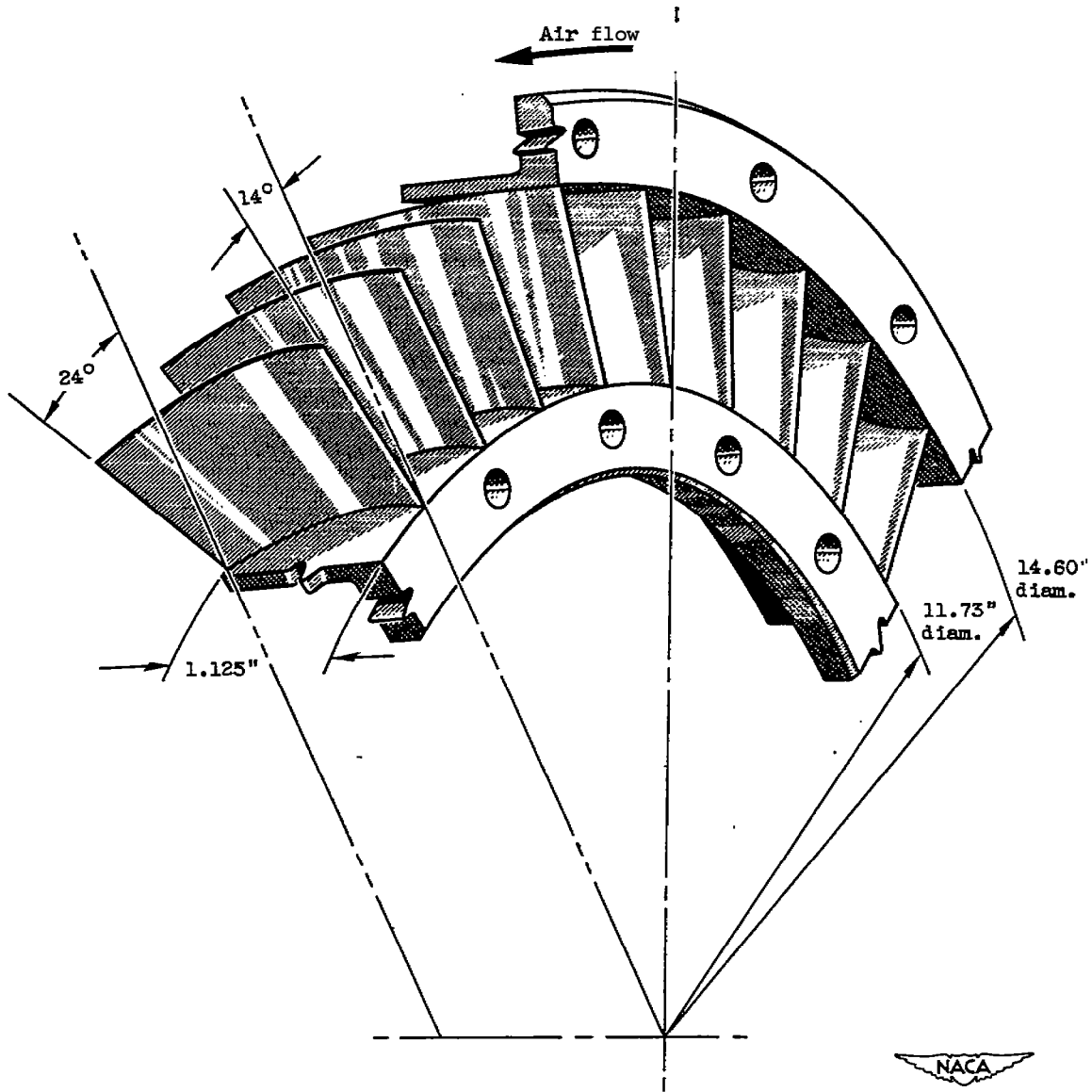


Figure 2. - Construction of stator-blade profile (mean section). (All dimensions in in.)

104



473-1568

Figure 3. - Stator assembly showing setting of blades and annulus dimensions.

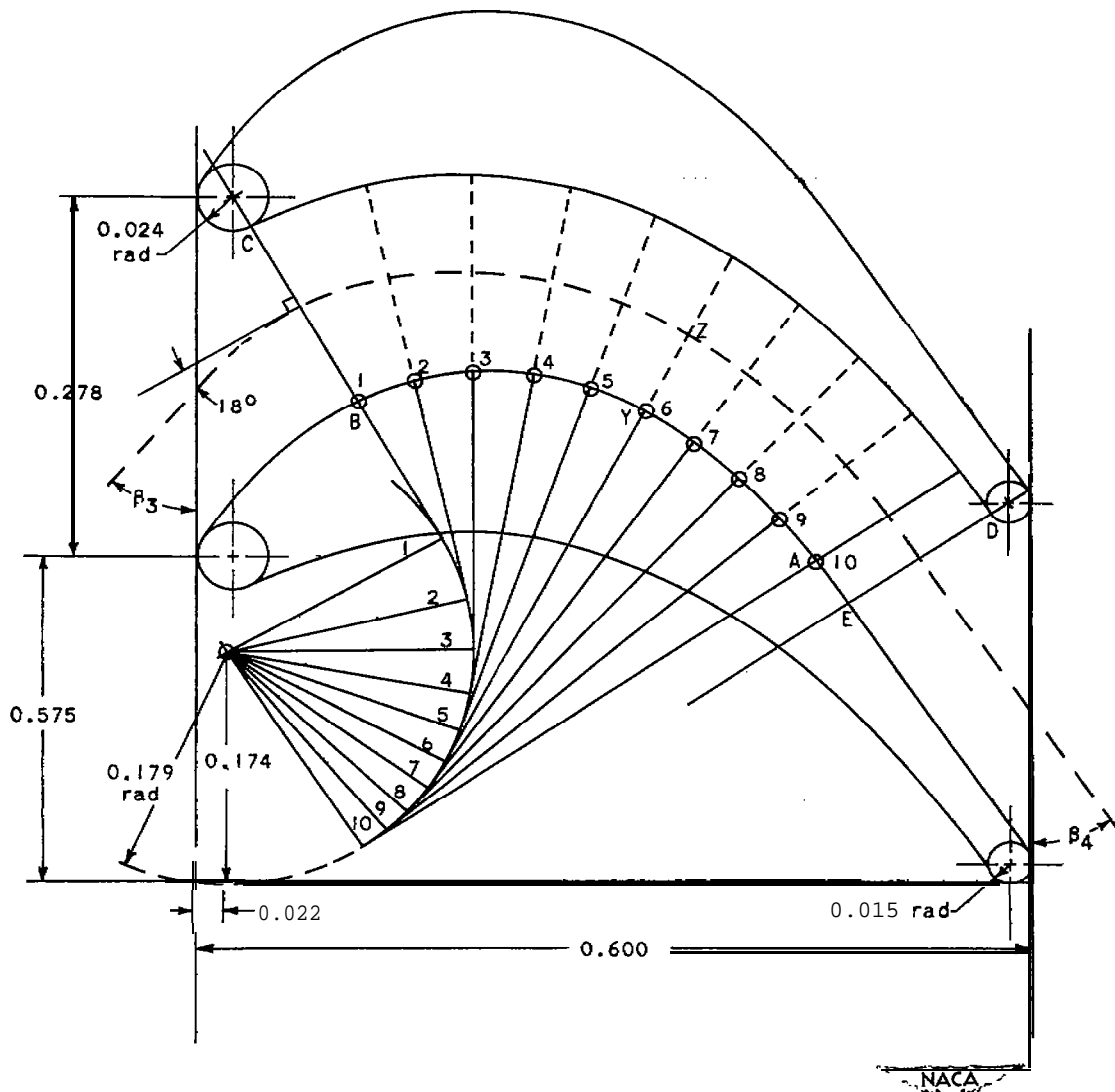


Figure 4. - Method of construction of rotor-blade profile (mean section).  
 (All dimensions in in.)

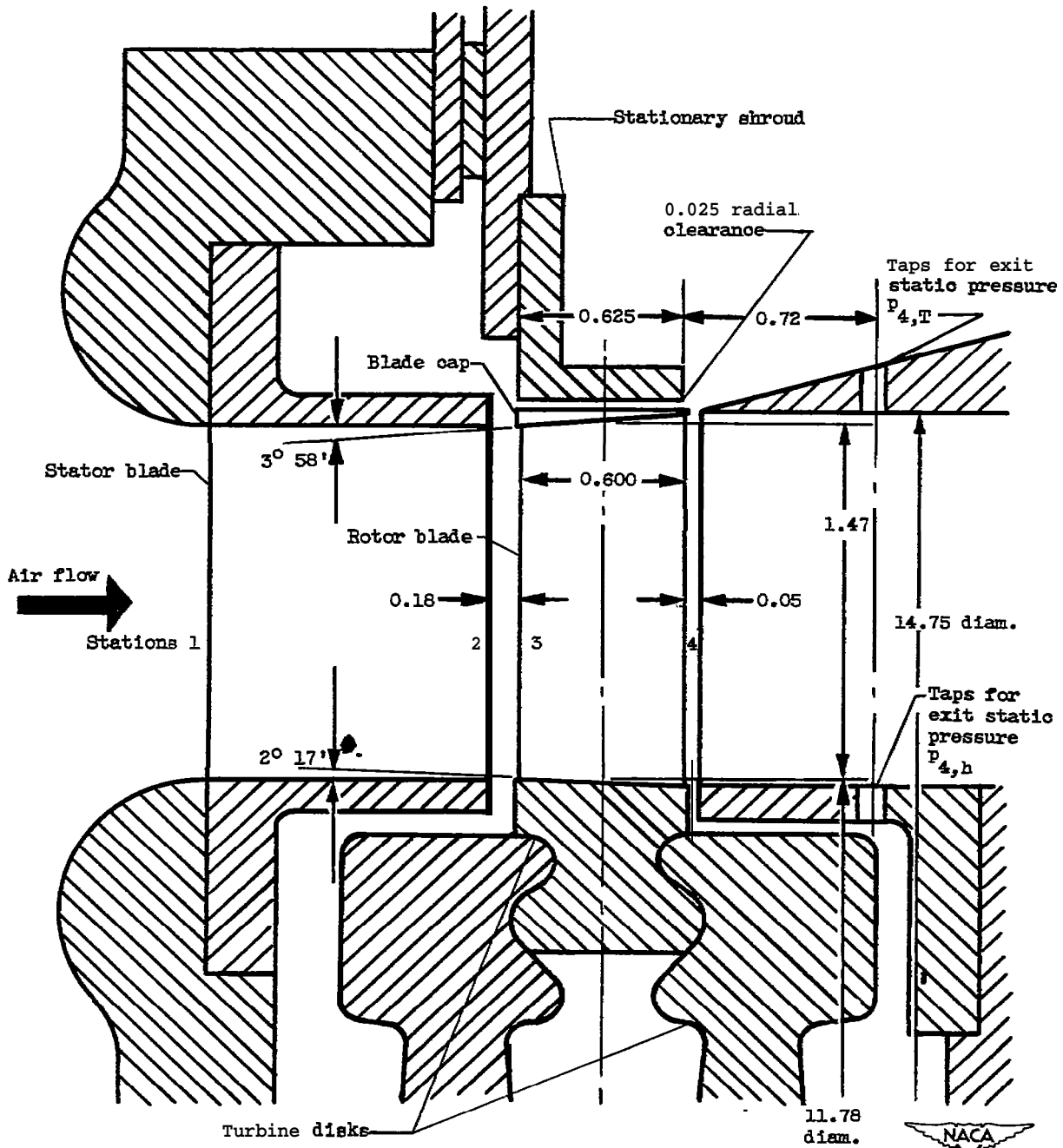
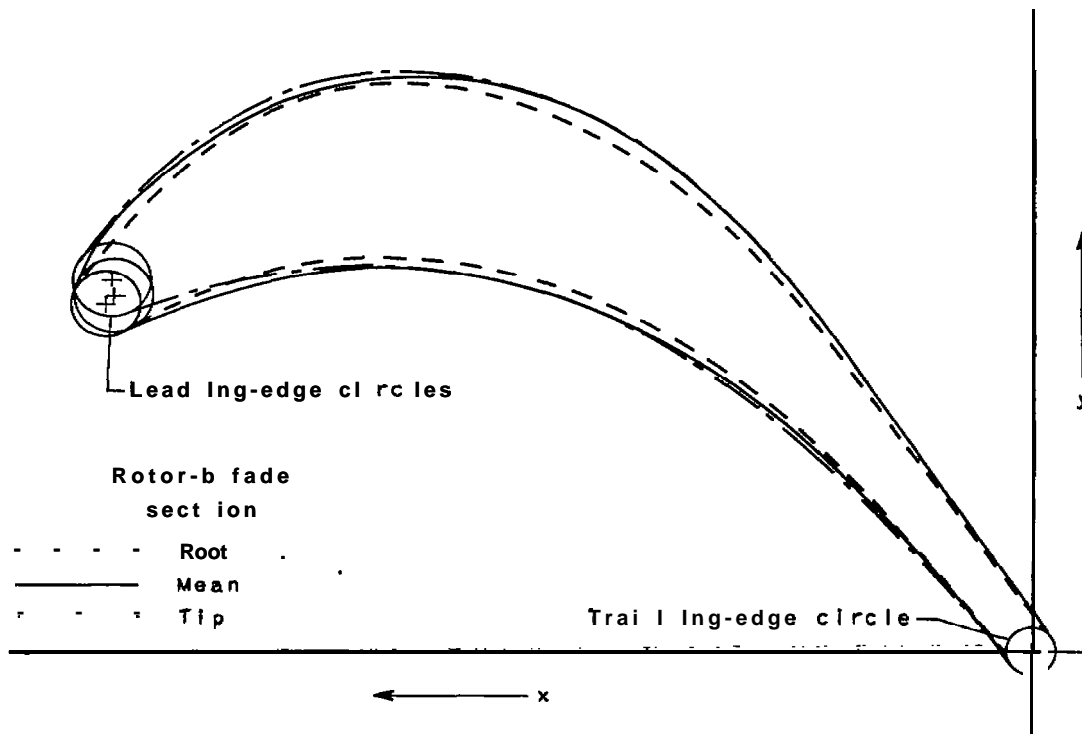


Figure 5. --Sketch of turbine-blading configuration showing turbine dimensions. (All dimensions in in.)

1104

4723-1569



	Position of leading-edge circle (in.)		Radius of circle (in.)	
			Leading edge	Trailing edge
	x	y		
Root	0.565	0.229	0.020	0.015
Mean	.560	.234	.024	.015
Tip	.561	.244	.023	.015

Figure 6. — Superimposed root, -mean, and tip sections of rotor blade.

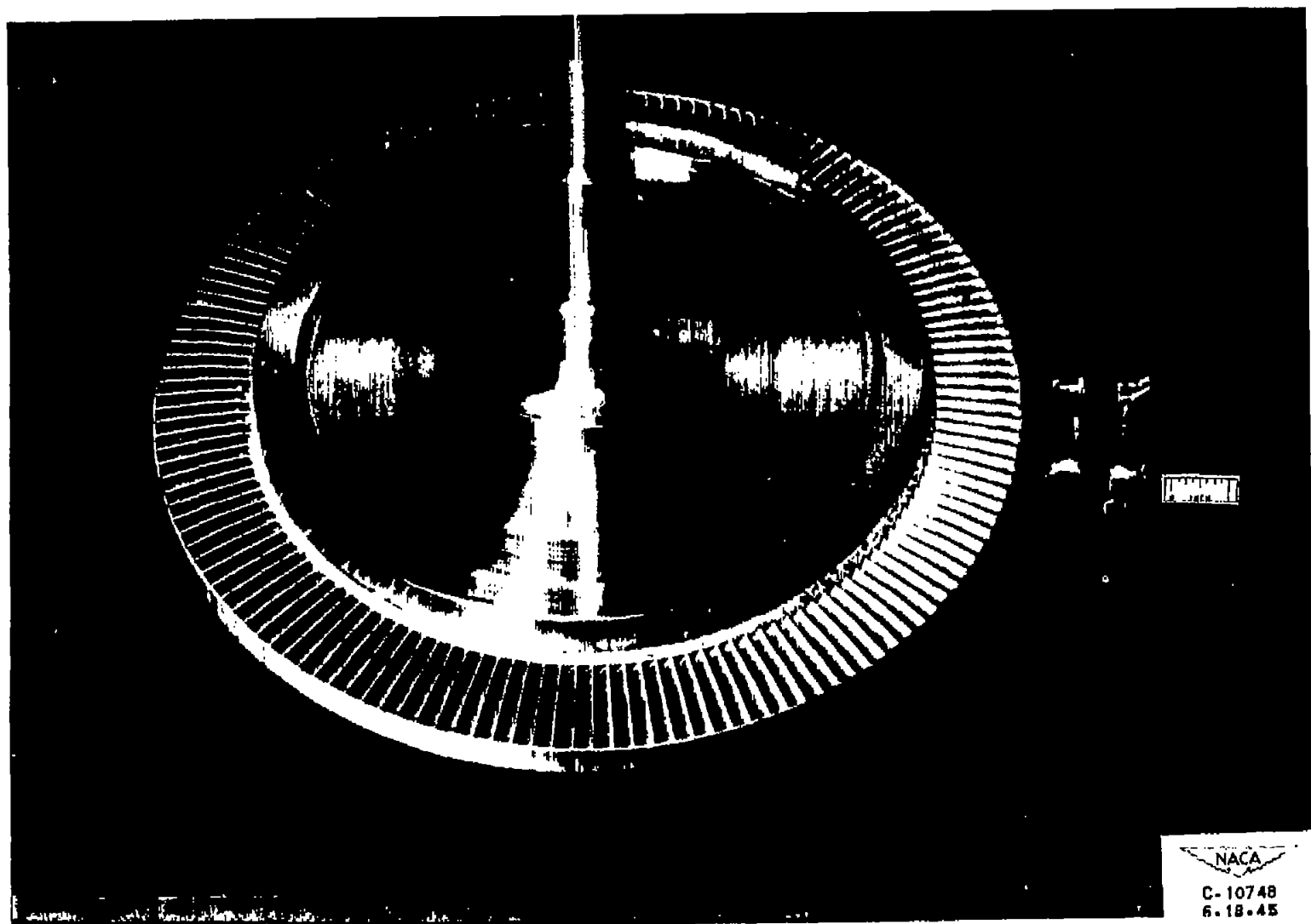


Figure 7. - Assembled rotor showing rotating shroud formed by blade caps.

1

2

3

4

5

6

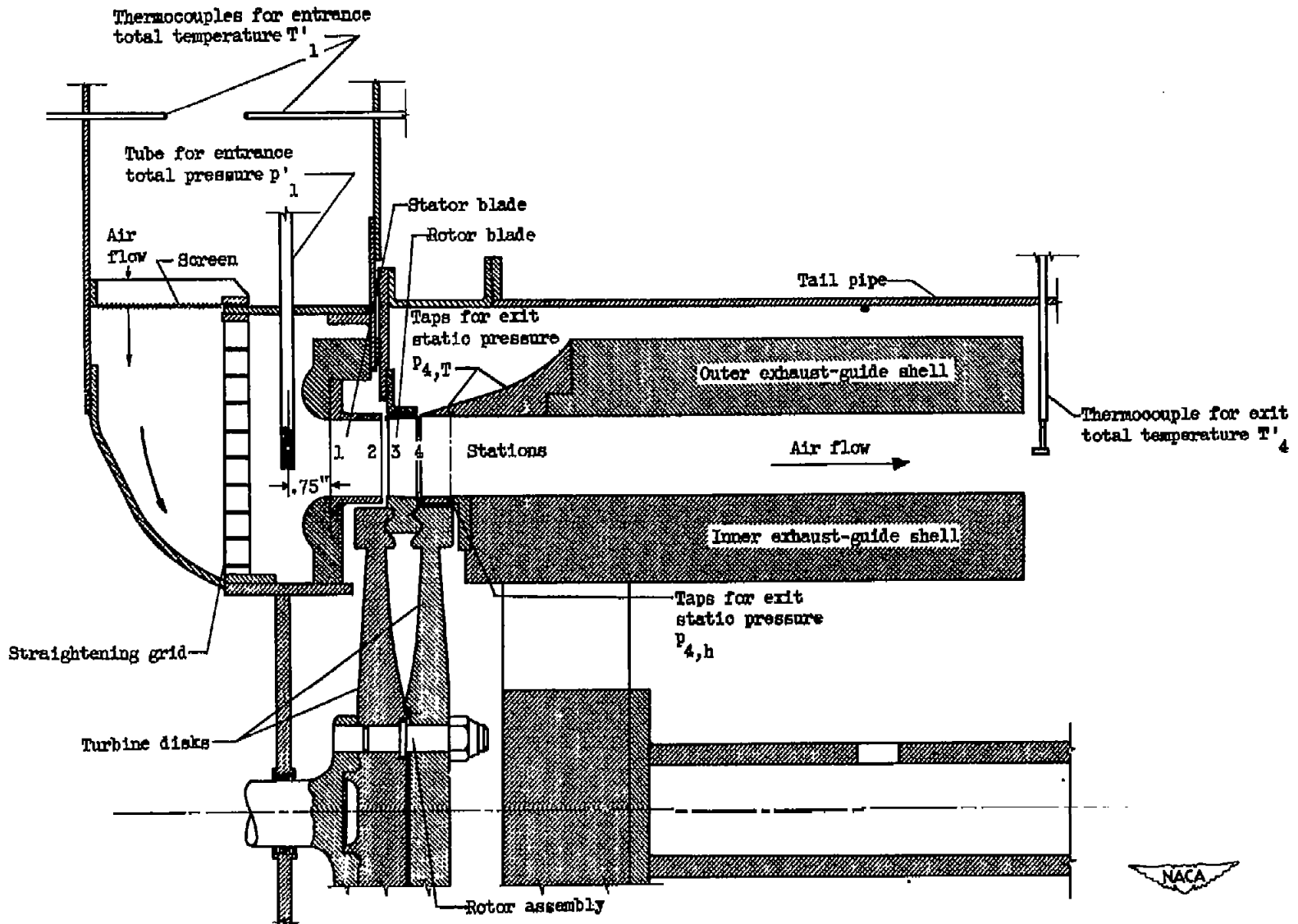


Figure 8. - Cross section of turbine assembly showing instrumentation.

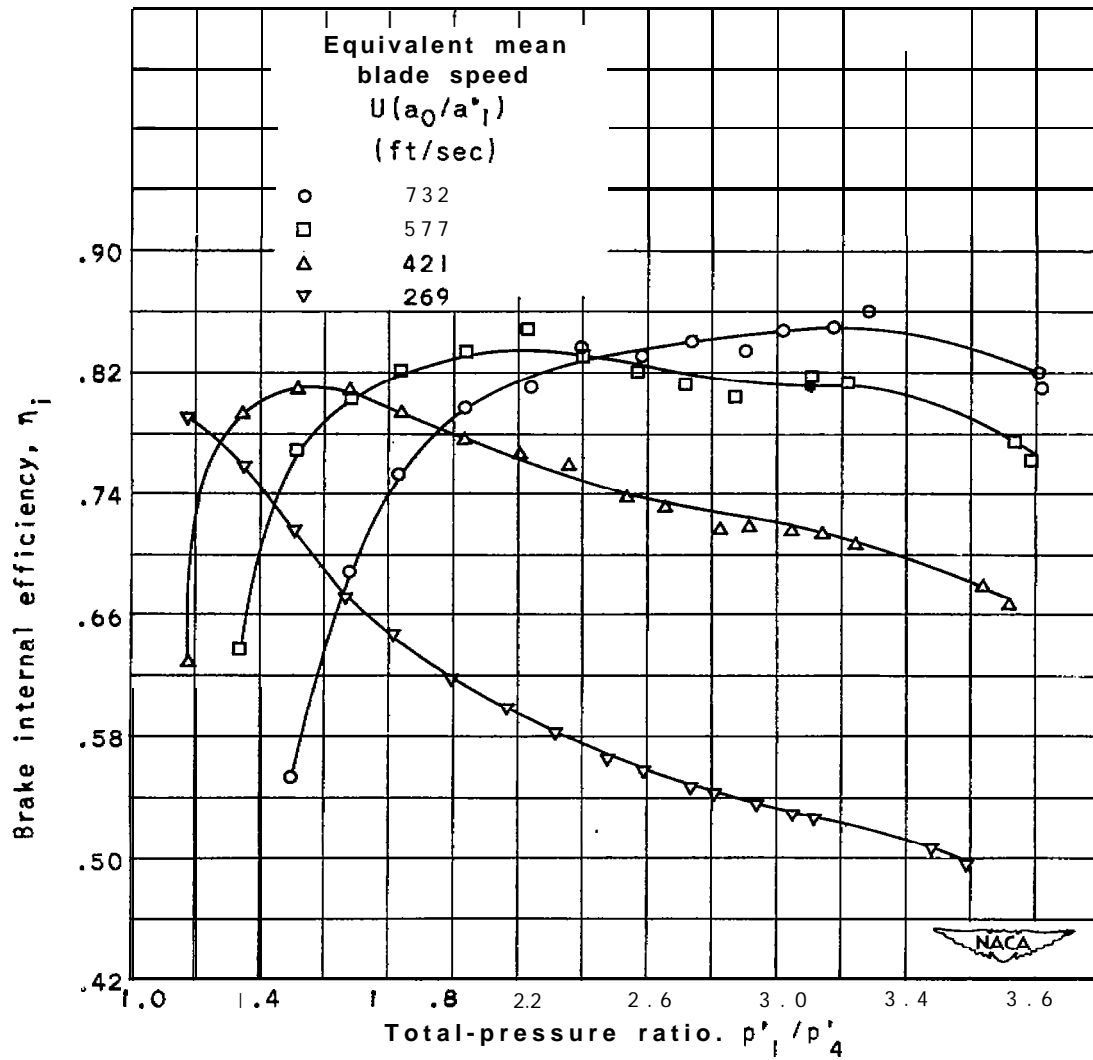


Figure 9. - Variation of brake internal efficiency with blade speed and total-pressure ratio.

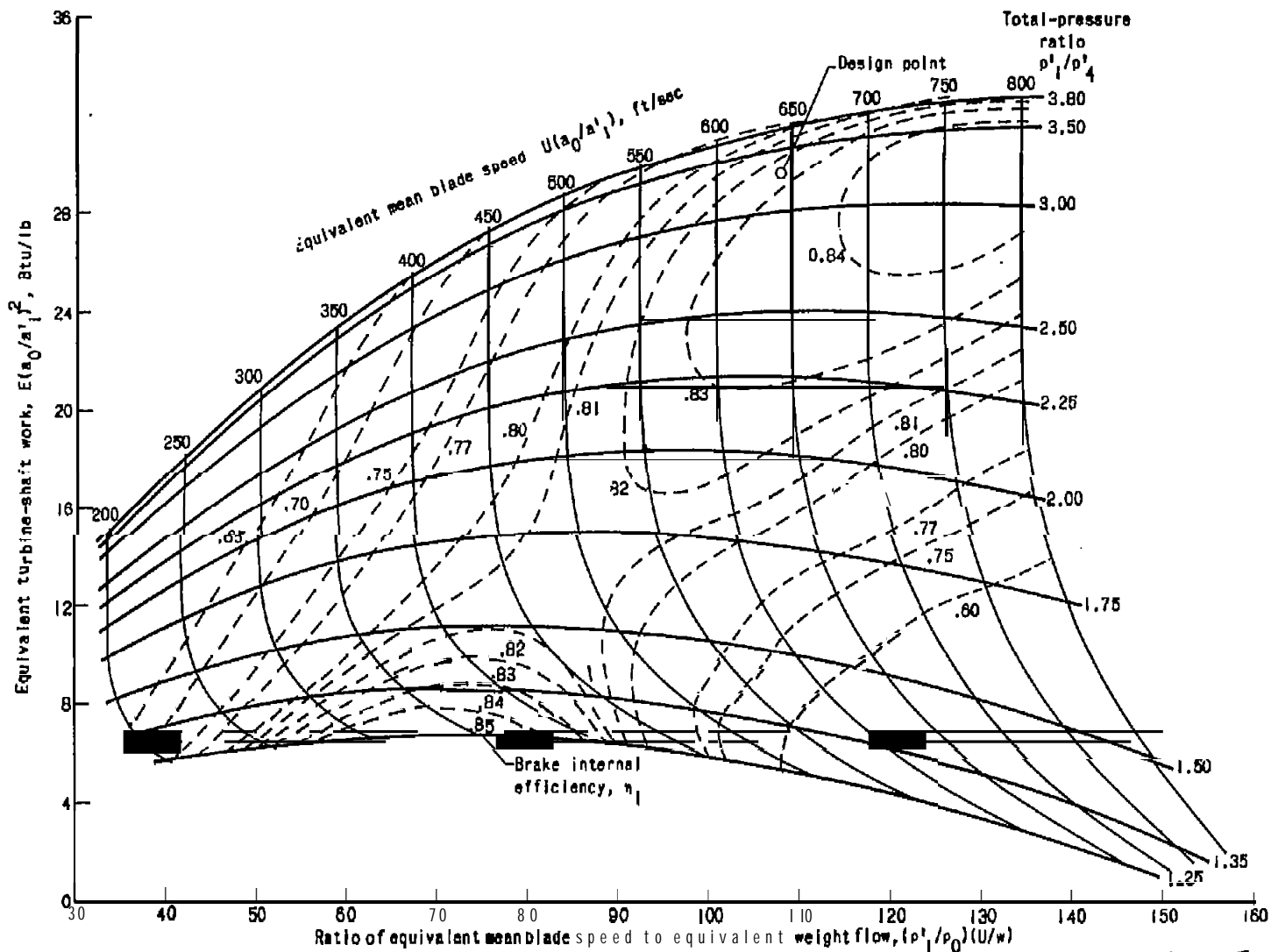


Figure 10. - Over-all turbine performance.



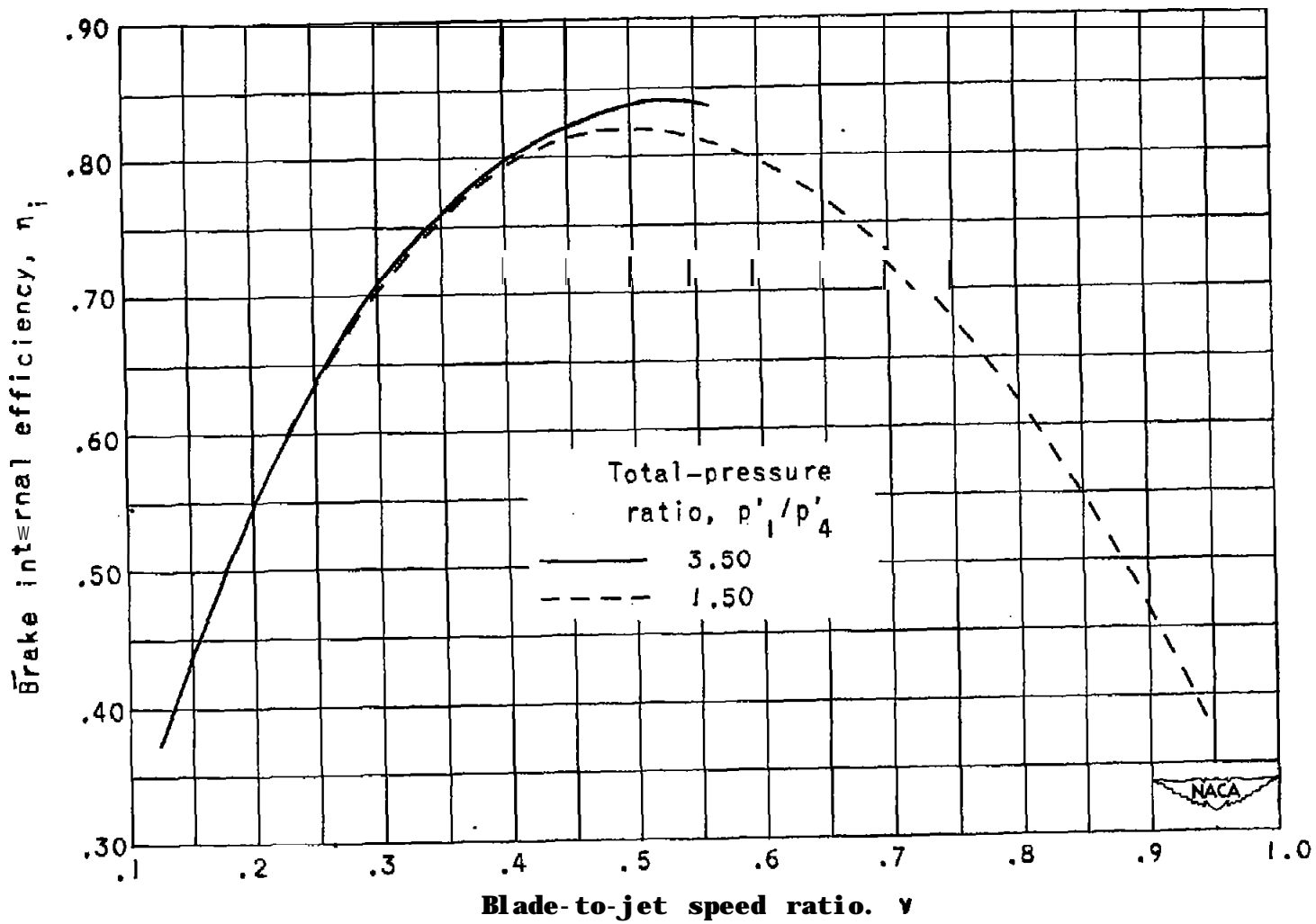


Figure II. - Variation of brake internal efficiency with blade-to-jet speed ratio.

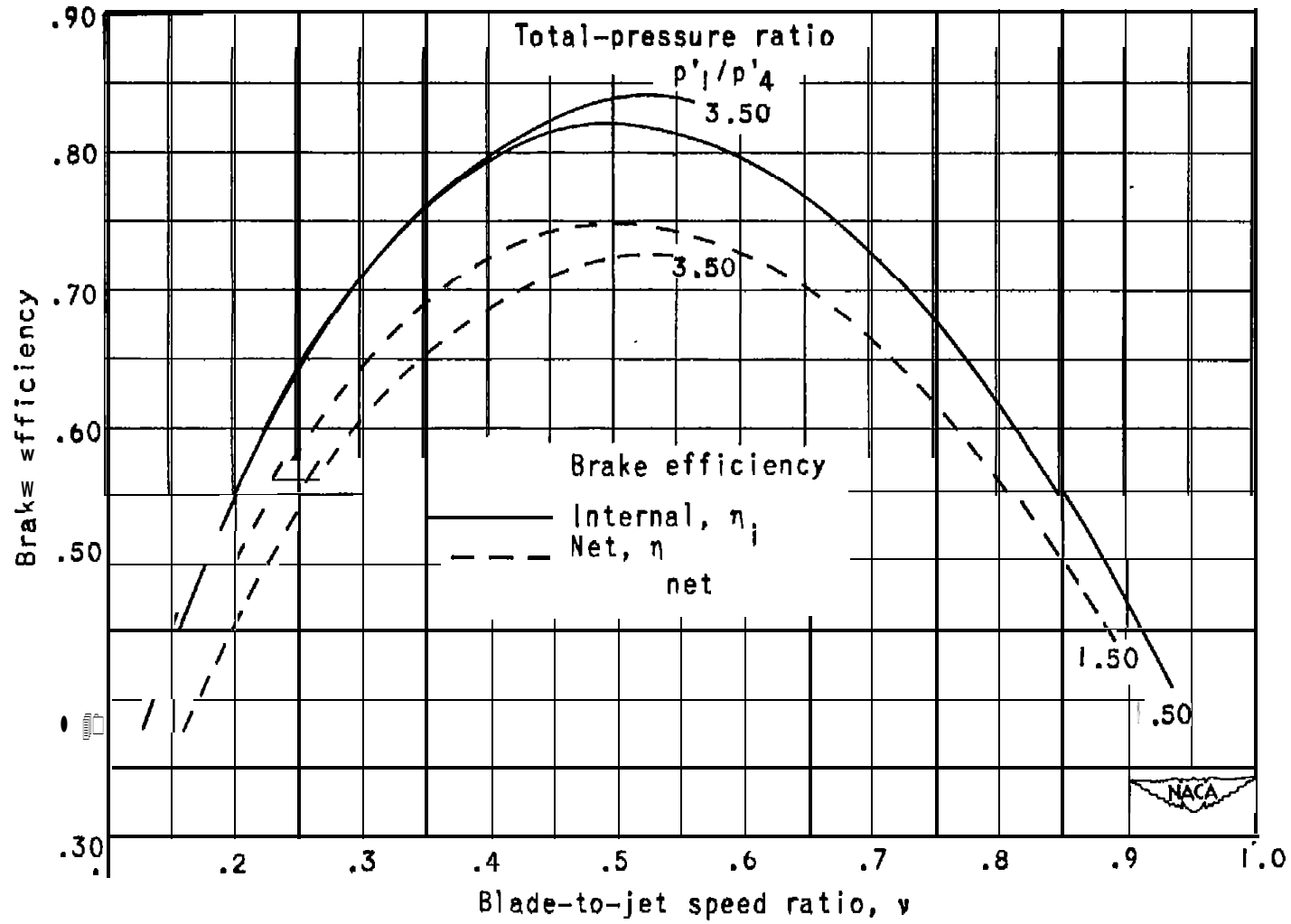


Figure 12. - Comparison of brake internal and brake net efficiencies.

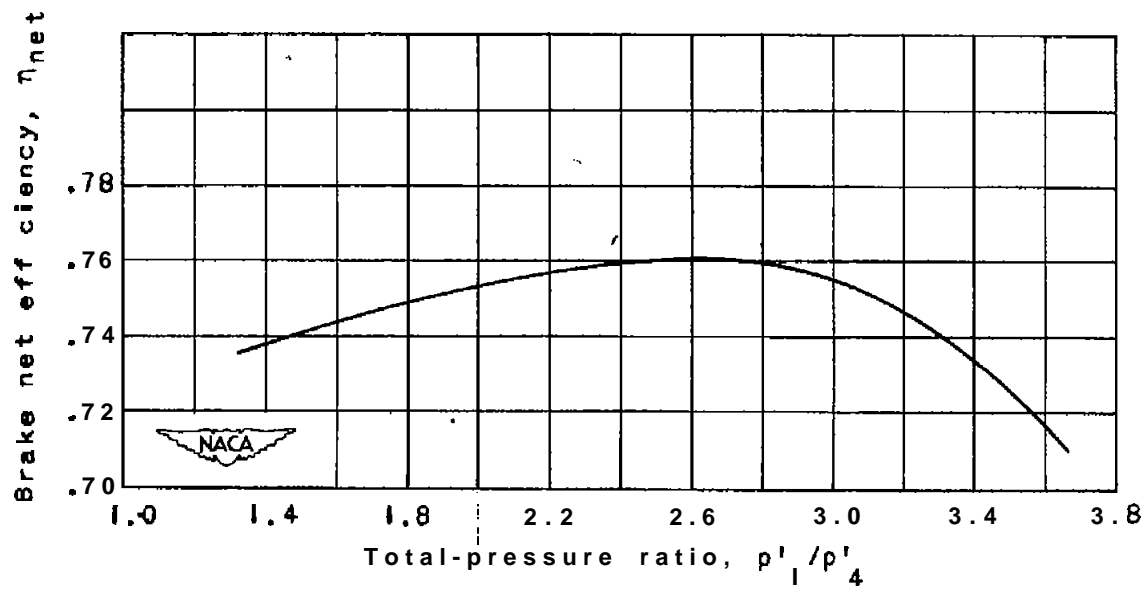


Figure 13. - Variation of brake net efficiency with total-pressure ratio. Blade-to-jet speed ratio, 0.54.

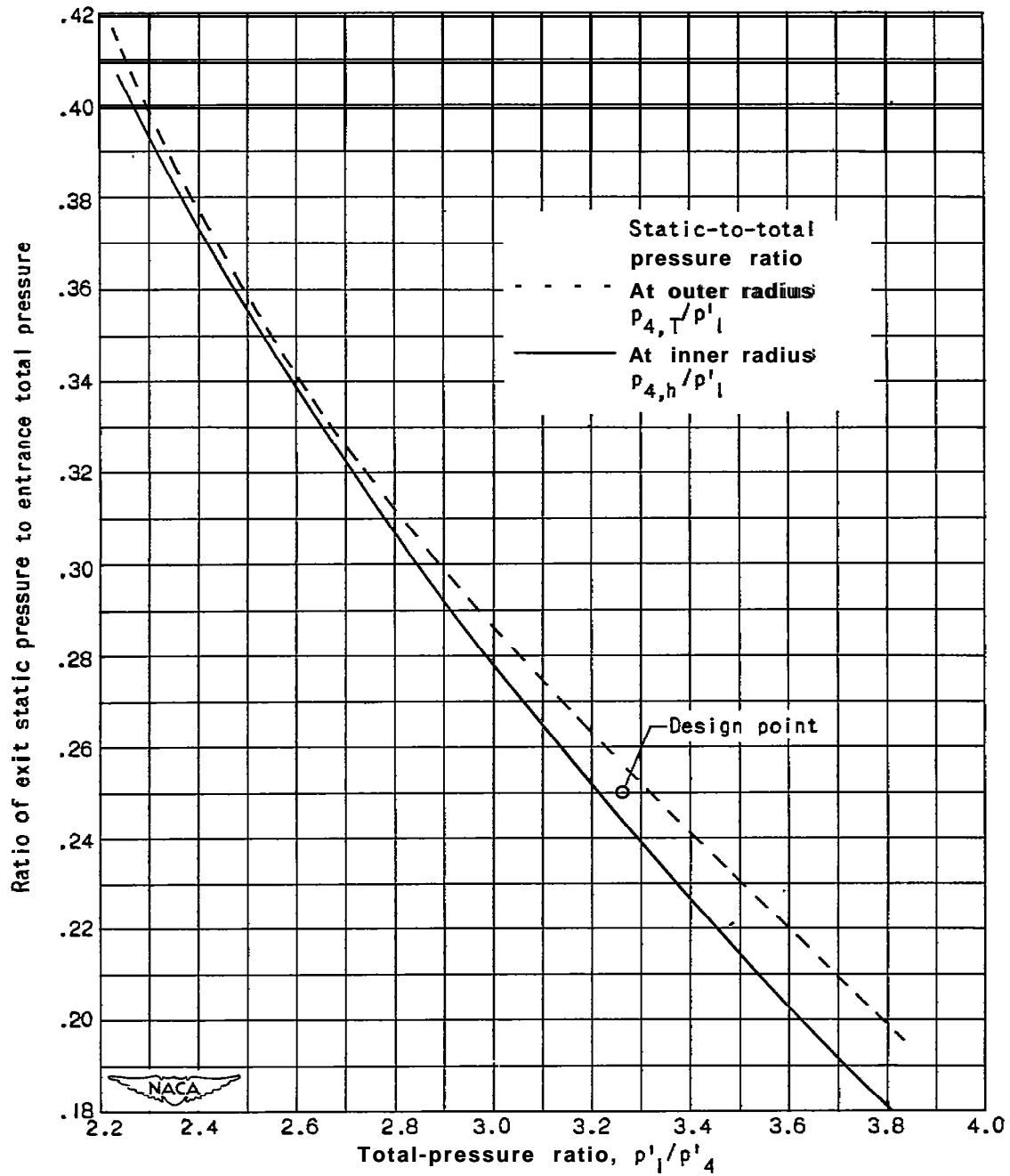


Figure i4. - Comparison of static pressures at inner and outer radii of annulus at rotor exit.

NASA Technical Library



3 1176 01435 0780